

Uniaxial incommensurate rare-gas-monolayer solids. II. Application to Xe/Pt(111)

J. M. Gottlieb and L. W. Bruch

Department of Physics, University of Wisconsin-Madison, Madison, Wisconsin 53706

(Received 28 February 1991)

An effective interaction model is reported for the interactions of xenon adsorbed on the (111) face of platinum. Many structural properties of the observed uniaxial incommensurate phase are reproduced. The uniaxial phase has a large linear thermal expansion and a commensurate triangular lattice becomes the minimum-free-energy phase at intermediate temperatures. A multiparameter monolayer interaction model, constructed from terms used for other physisorption systems, has too weak a short-range adatom-adatom repulsion. Analysis and reinterpretation of data for the heats of adsorption also show the need for an additional repulsive term.

I. INTRODUCTION

Monolayer xenon adsorbed on the (111) face of platinum, Xe/Pt(111), may provide the most complete range of commensurate and partial-registry structures observed in a classical physisorption system.^{1,2} Early attempts to model the monolayer solid found it surprisingly difficult to reproduce these structures.^{3,4} Recently, diffraction data for the uniaxial incommensurate (UIC) solid were reinterpreted⁵ as showing the need to consider a different class of adatom-substrate potentials for Xe/Pt(111). This paper presents an interaction model which yields many of the phenomena of the UIC solid. The analysis, based on the methods presented in the accompanying paper⁶ (I), also sharpens the puzzles posed by the remaining differences between the model calculations and the experimental data.

The uniaxial incommensurate monolayer solid is expected to be an important intermediate stage in a continuous commensurate to incommensurate phase transition.⁷ Also this is a relatively simple structure for studying the properties of domain walls⁸ because they are parallel on the average and effects of wall crossings are small. However, it is observed over an extended range of misfit in only two physisorption systems: molecular hydrogen on graphite⁹ and Xe/Pt(111).^{10,11} The Xe/Pt(111) monolayer is an excellent system for analysis because there are extensive experimental data and some simplifications arise for adsorbed xenon: (1) There is a well-established triangular commensurate solid.^{2,12} (2) There is a uniaxial incommensurate (UIC) solid phase which is stable for a wide range of mean misfit, $0 < \bar{m} < 6.5\%$.^{10,11} (3) There is a diffraction satellite demonstrating the strongly modulated character of the UIC solid at mean misfit less than 4%.^{10,11,13} (4) There are data for heats of adsorption, compressibility, and thermal expansion of the UIC solid.^{2,12,14} (5) Xenon is an atomic adsorbate which interacts primarily by pair potentials and which can be treated by classical statistical mechanics over much of the temperature range of the experimental data.¹⁵

There has been little modeling of the Xe/Pt(111)

monolayer. Black and co-workers^{3,4} performed molecular-dynamics simulations of small rafts of xenon atoms. Their first choices of parameters did not lead³ to a stable commensurate $(\sqrt{3} \times \sqrt{3})R 30^\circ$ lattice. They did obtain it later,⁴ but only by using a surprisingly large value of the leading Fourier amplitude of the adatom-substrate potential. Bethune, Barker, and Rettner¹⁶ constructed a xenon-platinum potential from atom-atom sums, which reproduced known features of the average potential and also led to a large leading Fourier amplitude. To do this they had to attribute a quite small van der Waals radius to the xenon atom. Tully and co-workers¹⁷ had previously constructed a xenon-platinum potential with a small barrier to surface diffusion. Hall *et al.*¹⁸ modeled the frequency spectrum of incommensurate monolayers and of bilayers and trilayers of inert gases on Pt(111), using conventional models for the adatom-adatom interactions.

Constructions of the adatom-substrate holding potential for the (111) face of a face-centered-cubic solid substrate from atom-atom sums¹⁹ usually lead to potentials for which the minima are at sites with threefold coordination to the substrate atoms. This is the case for the models used by Black and co-workers,^{3,4} Bethune, Barker, and Rettner,¹⁶ and Tully and co-workers.¹⁷ However, two independent and concurrent investigations^{5,20} of Xe/Pt(111) led to the proposal that the holding potential minima for the xenon are at sites atop surface platinum atoms. Gottlieb⁵ showed that an observed diffraction satellite^{10,13} for the UIC solid is absent for a holding potential model in which the two sets of threefold sites of the fcc (111) surface are degenerate energy minima, and that it is present for a model in which the minima are at atop sites. Müller²⁰ used local-density-functional theory to calculate the interaction of one and two xenon atoms with small clusters of platinum atoms and also concluded that the minima are at atop sites.

As shown in the accompanying paper,⁶ domain walls separating domains of atoms in the different threefold sites provide a low-energy mechanism for accommodating uniaxial misfit in a monolayer adsorbed on an fcc (111) substrate. Consequently, rather large Fourier amplitudes for the adatom-substrate potential are required

to stabilize the commensurate solid relative to the UIC solid; this is indeed the experience of Black and Janzen.⁴ However, as will be shown here, the required amplitudes are much smaller for the holding potential model with only one minimum per surface Bravais cell and the barriers to lateral motion inferred for the Xe/Pt(111) model are on the scale of those estimated for xenon on graphite.¹⁹ This is a surprising result^{15,21} in the light of previous ideas of metallic electrons smoothing the effective surface. Müller's calculation²⁰ indicates chemical hybridization has a role in the effective interaction.

The model for the Xe/Pt(111) monolayer consists of Lennard-Jones (12,6) pair potentials for the xenon-xenon interactions and a representation of the xenon-substrate interaction by a Fourier amplitude V_g for the lateral variation of the holding potential. The distinction between minima at atop sites and at threefold sites is set by the sign of V_g . For $V_g < 0$, the minima are at atop sites and, in this planar monolayer model,⁶ the barrier to lateral motion on the holding potential is $-8V_g$. In this model for Xe/Pt(111), the barrier is ~ 50 K, which is much less than the value inferred by Kern *et al.*² from isosteric heat data; it is close to the 40 K barrier found for the Morse potential model of Tully and co-workers.¹⁷ An important result of the analysis⁶ is that the increment in a thermodynamic function such as the chemical potential can be much larger than the single atom barrier because of the contributions from adatom-adatom interactions.

The model building has two parts. First, the UIC solid data of Kern and co-workers^{2,10,11,13} are used to narrow the range of interaction parameters in an effective interaction model. Second, a multiparameter potential model similar to that used¹⁵ for Xe/Ag(111) is constructed and applied for triangular lattices to test if the condensation energies can be understood. The thermodynamic analysis of the heats of adsorption²²⁻²⁴ is reviewed as part of the discussion of the data available^{2,12,14} for Xe/Pt(111).

The organization of this paper is as follows: The interaction models are described in Sec. II. An analysis of the data for the uniaxial incommensurate monolayer solid of Xe/Pt(111) is presented in Sec. III. An analysis of the heats of adsorption is presented in Sec. IV. Concluding remarks are presented in Sec. V.

II. INTERACTION MODELS

The interaction model for the UIC solid has the form treated in I.⁶ The adatom-adatom interactions are sums of Lennard-Jones (LJ) (12,6) pair potentials

$$\phi(r) = 4\epsilon[(\sigma/r)^{12} - (\sigma/r)^6] \quad (2.1)$$

and the adatom substrate potential, for motion restricted to the x - y plane, is

$$V(x, y) = -2V[\cos(g_0 x) + 2\cos(g_0 x/2)\cos(\sqrt{3}g_0 y/2)] \quad (2.2)$$

The choice of orientation of the adlayer coordinate axes relative to the substrate which was made in I is used in Eq. (2.2); the origin of coordinates is at a surface plat-

num atom. The amplitude V is related to V_g of I by $V = -V_g$.

Properties of the UIC solid are described for two sets of parameters: (a) $\epsilon = 230$ K, $\sigma = 4.05$ Å, and $V = 6$ K; (b) $\epsilon = 230$ K, $\sigma = 4.10$ Å, and $V = 3$ K. The energy scale is retained from models used²⁵ for Xe/Ag(111), and σ and V are adjusted to give a fair overall account of the structural properties of the UIC solid of Xe/Pt(111). Thus the parameter sets define effective interactions for the monolayer xenon. The conclusion here is that case (a) is a better model for Xe/Pt(111) than case (b); case (a) corresponds to a more modulated UIC solid than case (b). The extent to which the effective interaction does describe Xe/Pt(111) is noteworthy: from previous work with positive V_g , it appeared^{3,4,16} that it would be difficult to construct such a model from the ingredients ordinarily used in physisorption theory.

A multiparameter xenon-xenon interaction model is constructed in analogy to the procedure^{15,26} used for Xe/Ag(111), to compare with the fitted effective LJ (12,6) potential. The Barker X2 potential for isolated pairs in three dimensions is supplemented by the McLachlan substrate mediated interaction (parameters: $C_{s1} = 201$ a.u.; $C_{s2} = 154$ a.u.; $L = 2$ Å), the triple-dipole potential, and the interaction of the adsorption-induced polarizable dipoles. The single atom dipole moment μ_0 is taken to be 0.55 D, from the work-function change of 0.6 V reported by Schönhense.²⁷ The major change from the Xe/Ag(111) model is in the potential energy of the dipoles: for Xe/Pt(111) it is approximately twice as large as for Xe/Ag(111).²⁸

The length and energy scales of the Lennard-Jones pair potential and the multiparameter potential may be compared for the minimum-energy triangular lattice for $V = 0$, i.e., without substrate-registry effects. The minimum classical potential energy for the multiparameter model is -593 K per atom at a nearest-neighbor spacing of 4.41 Å. The corresponding energy for the LJ (12,6) model is -778 K per atom at a nearest-neighbor spacing in case (a) of 4.50 Å [case (b), 4.56 Å]. The differences in the nearest-neighbor spacings show that there is an additional repulsion incorporated in the effective potential which has not yet been identified for the multiparameter model. The multiparameter model has potential energy -469 K per atom at nearest-neighbor spacing 4.80 Å, corresponding to the $\sqrt{3} \times \sqrt{3}$ commensurate lattice of Xe/Pt(111).²⁹ The 124 K energy difference places a lower bound of 21 K on the value of V needed for the commensurate lattice to be the minimum energy structure at 0 K. However, as shown in paper I, if it is only required to be the minimum-free-energy structure at temperatures above 60 K, a much smaller value of V will suffice.⁶

III. COMPARISON TO DATA FOR UIC Xe/Pt(111)

The Xe/Pt(111) system was studied in a series of papers by Comsa and co-workers,^{1,2,10-14} using high-resolution atomic helium diffraction and inelastic scattering. Their data for the diffraction signature of the UIC lattice, the maximum misfit at low temperature, the iso-

thermal compressibility, and the domain of stability of the commensurate lattice relative to the UIC lattice are now discussed in terms of the interaction model.

A. Diffraction signature

Kern and co-workers^{10,11} and Zeppenfeld *et al.*¹³ reported observations of three (2, 3, and 4) of the five diffraction peaks enumerated in Fig. 1(a). The peaks 3 and 4 correspond to the average UIC lattice. A peak at position 2 is observed at small misfits, but not for misfit greater than about 4.0%. The calculated structure factors for case (a) are plotted in Fig. 1(b). These are evaluated for the configuration which minimizes the static potential energy of the UIC lattice at each value of mean misfit, as described in I.

A result of the model calculations^{5,6} is that the subdivided domain wall structure reported in I for the $V_g > 0$

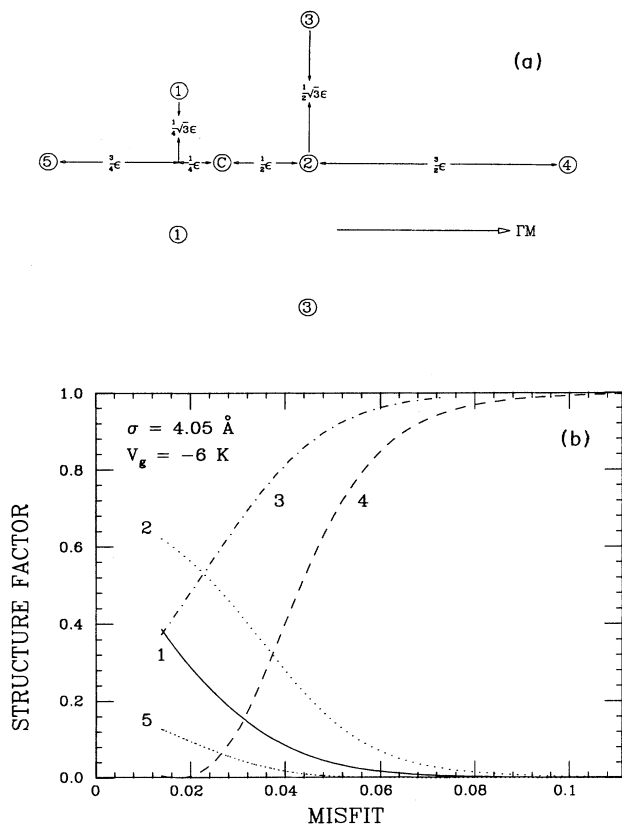


FIG. 1. Structure-factor calculations for UIC lattice as a function of mean misfit. (a) Wave-vector identifications. Positions of diffraction peaks in the neighborhood of the $(\sqrt{3} \times \sqrt{3})R30^\circ$ lattice peak (C) at $8\pi/3L$ for a three-domain average. Peaks near the ΓM axis, and axes at 120° and 240° to this axis, are shown, following Zeppenfeld *et al.* (Ref. 13). The scale ϵ is related to the mean misfit by $\epsilon = (8\pi/3L)[\bar{m}/(1-\bar{m})]$. The length L is the nearest-neighbor spacing in the substrate, $L = 2.77 \text{ \AA}$ for platinum. (b) Structure factors calculated for the case (a) interaction model, in the static planar lattice approximation.

cases leads to an extinction of the peak at position 2. It is not excluded yet that underlying layers of platinum atoms might break the degeneracy of the holding potential at the two sets of threefold sites to the extent there would be diffracted intensity at position 2. Models with distinctly different energies at the two threefold sites would be unusual for a physisorbed system.

The calculated structure factors for the $V_g < 0$ cases at small misfit have substantial intensity at position 2, and this intensity increases relative to the intensity at positions 3 and 4 as the magnitude of the misfit decreases. The calculations omit effects of thermal averaging and of multiple scattering corrections for the atomic probe, so that quantitative comparisons with the experimental data are not possible. It does appear that smaller values of σ and larger values of V than those used for cases (a) and (b) would lead to more modulated UIC lattices, with substantial intensity at position 2, over a larger range of misfit than occur for UIC Xe/Pt(111).

B. Maximum misfit of the UIC lattice at condensation

At temperatures below about 60 K, the monolayer solid of Xe/Pt(111) condenses in the UIC lattice.¹ The misfit at condensation increases as the temperature decreases^{2,10,11} and at the lowest temperature reached in the experiments, 25 K, it is 6.5%. The misfit of the minimum-free-energy UIC lattice at 25 K, calculated in the quasiharmonic approximation, is 6.4% for case (a) and 5.0% for case (b).

C. Stability of the commensurate lattice

The Xe/Pt(111) monolayer condenses into a triangular commensurate $(\sqrt{3} \times \sqrt{3})R30^\circ$ lattice in the temperature range $62 < T < 99 \text{ K}$.^{1,2} The transition to the UIC lattice is continuous for condensation at a temperature near 60 K (Refs. 1 and 2) and after a finite increase in chemical potential at temperatures above 62 K.² Figure 9 of paper I presents a phase diagram in chemical potential and temperature coordinates for case (a) which displays such a domain of stability of the commensurate lattice.

The quasiharmonic lattice approximation is known^{25,30} to overestimate the thermal expansion for triangular lattices of xenon at temperatures above 60 K. The initial temperature for condensation into the commensurate lattice thus is taken to be 50 K for the quasiharmonic theory, in an attempt to compensate for this failing. The threshold amplitudes V , in quasiharmonic approximation, are then 5.3 K for $\sigma = 4.05 \text{ \AA}$ and 2.9 K for $\sigma = 4.10 \text{ \AA}$. The parameters of cases (a) and (b) correspond to models in which the UIC lattice thermally expands into the commensurate lattice at temperatures in the range 50–60 K. The calculated thermal expansion of these UIC lattices, i.e., the variation of the mean misfit, is twice as large as the calculated linear thermal expansion of triangular lattices of Xe/Ag(111).^{15,25,30}

Kern *et al.*² reported values for the isosteric heat and the partial molar entropy in the region of the commensurate-incommensurate transition, at temperatures of 85–95 K. They fitted data for the temperature

dependence of the three-dimensional (3D) gas pressure to the form

$$\ln p = -q_{st}/k_B T + b(\theta) \quad (3.1)$$

and found decreases $\Delta q_{st} = -30$ meV and $\Delta b/k_B = -3$ to -4 in the region of the transition.

The increment in chemical potential from monolayer condensation to the commensurate-incommensurate phase transition is then

$$\Delta\mu = -\Delta q_{st} + k_B T \Delta b. \quad (3.2)$$

The data² correspond to an increment $\Delta\mu$ which decreases with increasing temperature, while the quasiharmonic theory leads to a $\Delta\mu$ which increases with increasing temperature. This is the most serious contradiction between the model and the data and is not yet understood. The domain-wall meanderings,^{7,8} not well treated by the small-amplitude vibration theory, may be a significant contribution to the entropy. It may be that experimental data closer to the phase transition are required and that the difference in 3D gas temperature and substrate temperature becomes important in this context.

The value of $\Delta\mu$ at 70 K is 210 K for both cases (a) and (b). Thus the commensurate phase is stable over a considerable range of chemical potential in the model calculation.

D. Isothermal compressibility

The monolayer isothermal compressibility has been recalculated from data^{2,31} for the misfit of the UIC lattice as a function of the 3D gas pressure at constant temperature ($T=88$ K). The value ranges from 2.3×10^{-3} K/Å² at 4.7% misfit to 1.1×10^{-3} K/Å² at 7.0% misfit.

The calculated compressibility for the UIC lattice depends on terms corresponding to wall-wall interactions.⁶

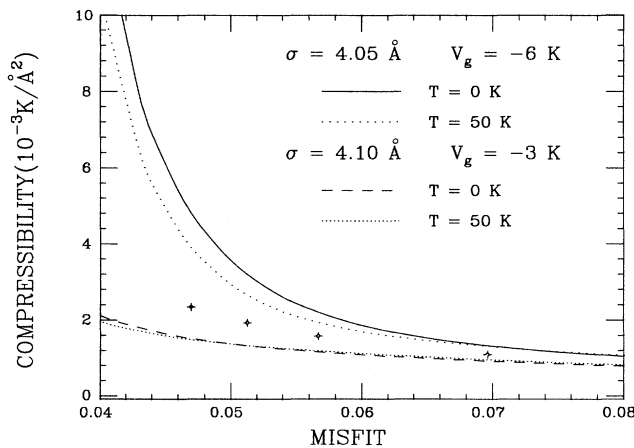


FIG. 2. Compressibility of the uniaxial incommensurate monolayer solid of Xe/Pt(111). Circles denote values derived from a reanalysis of the data of Kern and co-workers (Refs. 2 and 31) for the misfit as a function of pressure at 88 K. The solid and dashed lines denote values calculated for the case (a) and (b) effective interactions with the quasiharmonic approximation at 50 K.

At small misfits, the compressibility is large, and for a system of very narrow domain walls, it remains large for larger misfits. The calculated compressibility at 0 and 50 K for the two cases is shown in Fig. 2, with the reanalyzed data: the values for the models lie in the range of the data. Models with $\sigma=4.0$ Å and with larger magnitudes of V led to narrower domain walls and to compressibilities much larger than the experimental values.

IV. HEATS OF ADSORPTION

The analysis⁶ of I emphasizes the structure and length scales of the UIC lattices. The heats of adsorption^{12,14} include measures of the monolayer binding energy and thus provide information on the energy scale of the effective interactions. This section includes a generalization of the thermodynamic analysis of the heats of adsorption²²⁻²⁴ to the case where the dense surface phase is a commensurate lattice.

The monolayer is treated as a phase in coexistence with an ideal 3D gas of chemical potential μ . The condition for thermodynamic equilibrium is that the grand potential

$$\Omega = F_{\bar{N}} - \mu \bar{N} \quad (4.1)$$

is minimum for the adsorbed phase of \bar{N} adatoms in specified area A and temperature T ; F is the Helmholtz free energy. The temperature, chemical potential, and grand potential of coexisting monolayer phases are equal. The grand potential is expressed in terms of the grand partition function by

$$\Omega = -(1/\beta) \ln \text{Tr} \exp[-\beta(H - \mu N)], \quad (4.2)$$

with $\beta = 1/(k_B T)$.

A. Heat of sublimation

Poelsema, Verheij, and Comsa¹² defined a heat of sublimation of the monolayer solid in terms of the temperature variation of the density of the 2D gas in coexistence with the solid:

$$q_{\text{sub}} = -d \ln(N_g / \beta A) / d\beta|_{\text{coex}}. \quad (4.3)$$

The monolayer heat of condensation is defined²³ in terms of the temperature variation of the pressure of the coexisting 3D gas:

$$q_1 = -d \ln p / d\beta|_{\text{coex}}. \quad (4.4)$$

The 3D gas is an ideal gas under the experimental conditions of monolayer Xe/Pt(111). Therefore the relation of the pressure to the chemical potential is known and Eq. (4.4) can be rewritten as

$$q_1 = \frac{5}{2}\beta^{-1} - d(\beta\mu) / d\beta|_{\text{coex}}. \quad (4.5)$$

The 2D gas is of low density and nearly ideal for most of the temperature range of Xe/Pt(111). Then a truncated virial series²⁴ for the chemical potential is

$$\beta\mu = \ln(N_g / z) + 2(N_g / A)B_2(T), \quad (4.6)$$

and for the grand potential is

$$\Omega = -N_g k_B T [1 + (N_g/A) B_2(T)] . \quad (4.7)$$

The one-atom partition function z in Eq. (4.6) is given by

$$z = \text{Tr} \exp\{-\beta[p^2/2m + u(\mathbf{r})]\} , \quad (4.8)$$

with kinetic energy and holding potential $u(\mathbf{r})$; in the classical limit z is proportional to a configuration integral for motion parallel and perpendicular to the planar substrate surface. The second virial coefficient B_2 , for a two-particle cluster in the presence of a spatially periodic holding potential,²⁴ is not evaluated in this work.

Let $\langle H_s \rangle$ denote the average internal energy of the monolayer solid and $\langle h_g \rangle$ the average internal energy per atom of the low-density 2D gas. The heat of sublimation Eq. (4.3) is

$$q_{\text{sub}} = \beta^{-1} - [1 - (2N_g B_2/A)] \\ \times (\langle H_s \rangle - N_s \langle h_g \rangle) / (N_s - N_g) \\ + (N_g/A) dB_2(T)/d\beta , \quad (4.9)$$

where the coexisting phases have number density N_s/A and N_g/A . The energy $\langle h_g \rangle$ is

$$\langle h_g \rangle = -d \ln z / d\beta + (N_g/A) (dB_2/d\beta) . \quad (4.10)$$

The corresponding expression for q_1 is

$$q_1 = \frac{5}{2} k_B T - (\langle H_s \rangle - N_g \langle h_g \rangle) / (N_s - N_g) . \quad (4.11)$$

The truncated virial series for the low-coverage isosteric heat is

$$q_{st} = \frac{5}{2} \beta^{-1} + d \ln z / d\beta - 2(N_g/A) dB_2/d\beta . \quad (4.12)$$

The second virial contributions are included in Eqs. (4.9)–(4.12) to emphasize the possible importance of gas imperfection terms when data for the heats of adsorption are used to estimate monolayer cohesive energies, even if the 2D gas density is only a few percent of the solid density. The area per adatom of monolayer solid xenon is of order 18 \AA^2 . The second virial coefficient for the Xe/Ag(111) system at 90 K was estimated to be -100 \AA^2 per atom.¹⁵ Then the product $B_2 N_g/A$ is of order -0.05 already when the 2D gas has density 1% of the solid density. The corresponding term in the isosteric heat, Eq. (4.12), is 80 K/atom .¹⁵

If all gas imperfection terms are neglected in Eq. (4.9), the sublimation energy becomes

$$q_{\text{sub}} = \beta^{-1} + d \ln z / d\beta - (\langle H_s \rangle / N_s) . \quad (4.13)$$

For the nearly two-dimensional models used in this work, the laterally averaged holding potential and perpendicular vibration energies cancel between the gas and solid energy terms in Eq. (4.13). Thermal equipartition energies of $2k_B T$ for the 2D solid and $1k_B T$ for the kinetic energy of the 2D gas cancel with the leading term on the right-hand side of Eq. (4.13). The corrugation potential-energy contribution to the 2D gas energy is -3 K (-1 K) for $V=6 \text{ K}$ of case (a) [$V=3 \text{ K}$ of case (b)] at 90 K; in both cases it is a small part of the net sublimation energy. For

an amplitude $V = -60 \text{ K}$, which is the scale found⁶ in I to stabilize commensurate lattices with domains in three-fold sites, the contribution to the 2D gas potential energy is -113 K ; this is a significant offset to the registry potential (then -180 K) in $\langle H_s \rangle$. For the case (a) and (b) models, the conclusion is that the heat of sublimation directly gives the potential energy of the commensurate lattice in a temperature range where the 2D gas is nearly ideal.

The values for the heats of adsorption for Xe/Pt(111) used in Sec. IV B are $q_{\text{sub}} = 550 \pm 50 \text{ K}$ at temperatures of $82\text{--}92 \text{ K}$;¹² $q_1 = 311 \pm 16 \text{ meV}$ ($3610 \pm 190 \text{ K}$) at temperature $85\text{--}100 \text{ K}$.¹⁴ The low coverage isosteric heat is $q_{st} = 277 \text{ meV}$ (3210 K).¹⁴

B. Heat of bilayer condensation

A limit to the compression of the Xe/Pt(111) monolayer solid is set by formation of a bilayer solid.³² The most compressed monolayer has a triangular lattice and displays a small Novaco-McTague rotation.² The difference between the chemical potentials at monolayer and bilayer condensation gives a measure of the lateral stress in the compressed monolayer.

The reported value of the bilayer heat of condensation is $205 \pm 12 \text{ meV}$ at temperatures of $55\text{--}60 \text{ K}$.¹⁴ This is much farther removed from the 161 meV heat of sublimation of the bulk xenon solid than the value $173 \pm 5 \text{ meV}$ for Xe/Ag(111).²⁸ However, the lattice constants of the monolayer and the bilayer are equal¹⁴ to within the 0.01 \AA experimental accuracy, as for Xe/Ag(111). Then a previous argument³² applies and the chemical potential at the bilayer condensation should be only weakly dependent on the (strong) first layer holding potential. In fact, the pressure-temperature data¹⁴ of the Xe/Pt(111) bilayer condensation fall in the range of the corresponding data³² for Xe/Ag(111) and Xe/graphite. Thus the chemical potential at bilayer condensation for these three systems is very similar.

Therefore, for the following discussion, two values are used for the 2D enthalpy of the monolayer solid at bilayer condensation: 72 meV (840 K), from the difference between the reported¹⁴ bilayer heat of condensation and the low coverage isosteric heat; and 104 meV (1200 K), using the difference of the Xe/Ag(111) bilayer heat²⁸ and the low-coverage Xe/Pt(111) isosteric heat. The second value may be the better guide³² to the 2D enthalpy of the strongly compressed monolayer.

C. Monolayer energies

The potential energy for a triangular lattice with nearest-neighbor spacing 4.80 \AA is -469 K/atom for the multiparameter interaction model described in Sec. II. For $V = 10\text{--}20 \text{ K}$, which is a range which would be estimated by analogy with the energy balances and thermal excitation effects found for the Lennard-Jones models,^{5,6} there would be an additional registry potential energy of -50 to -100 K per atom. The total potential energy of -520 to -570 K is in the range of the sublimation energy 550 K reported by Poelsema, Verheij, and Comsa.¹²

However, q_{sub} may overestimate the potential energy of the commensurate lattice by 10% as a result of the 2D gas corrections described in Sec. IV A.

The total potential energy per atom in the commensurate lattice for the Lennard-Jones interaction models, including the registry terms, is -734 K for case (a) [-740 K for case (b)]. To bring the energy to the range of the sublimation energy would require scaling the ϵ down by 25%; this is not an implausible amount in the light of known adsorption-induced modifications of gas-phase interactions.²⁶

An estimate of the lattice constant in the fully compressed monolayer can be made from potential-energy calculations and an identification of the increment $q_2 - q_{st}$ of 840 K (or, adjusted, 1200 K) with the 2D enthalpy. For the multiparameter interaction model it is 4.26 Å (or 4.22 Å), distinctly less than the observed limit of 4.33 Å.¹⁴ Adding zero-point-energy terms increases the calculated lattice constant by $\frac{1}{2}\%$; the lattice is still too compressed. This and the 4.41-Å lattice constant calculated for the minimum-potential-energy adlayer are evidence that a component of short-range repulsion is missing from the interaction model. The larger adsorption-induced dipole moment²⁷ for Xe/Pt(111) also indicates that there is a different adatom/substrate complex than for Xe/Ag(111). There has not yet been a determination of the effects in the lateral interaction which would correspond to the hybridization effects which Müller²⁰ noted in his calculation of the Xe/Pt(111) interaction.

The corresponding classical potential calculations for the Lennard-Jones models, cases (a) and (b), are easily done in terms of known lattice sums. For case (a) the most compressed monolayer has a lattice constant 4.33 Å at enthalpy 840 K and 4.30 Å at enthalpy 1200 K; the values for case (b) are 0.05 Å larger. If the calculations are repeated with the energy parameter scaled to 0.75ϵ , the lengths are reduced by 0.02 Å. Zero-point-energy terms will increase the classical lengths by $\frac{1}{2}\%$. The conclusion of this discussion is that the effective interactions lead to fully compressed monolayers with spacings in the range of the 4.33 Å experimental value.

V. CONCLUDING REMARKS

The effective interaction models, cases (a) and (b), lead to a fair degree of agreement with the experimental data for the UIC lattice of Xe/Pt(111). This is particularly satisfying because the Xe/Pt(111) monolayer had previ-

ously appeared to be a rather unusual physisorption system. Finding these models depended on recognizing⁵ that the diffraction data^{10,13} have a signature which excludes holding potential models with degenerate minima in the two sets of threefold sites.

The experimentally observed² decrease in the isosteric heat of adsorption at the commensurate-to-incommensurate monolayer phase transition is not easily interpreted as a chemical potential increment needed to drive the transition by compression. The calculations and the experimental data give opposite trends for the dependence of the chemical-potential increment on the temperature. More extensive computations, such as Monte Carlo simulations,¹⁵ might lead to a more accurate treatment of thermal excitations in the solid. Further experimental work might investigate the transition region more fully at smaller values of misfit.

The smallest atomic separations in the calculated UIC lattices, in the center of the domain walls, are smaller than the nearest-neighbor spacings in the corresponding zero-pressure 3D solids. This suggests a need to include 3D motions³³ into refined models of the UIC monolayer.

This work has not established the stability of the UIC monolayer relative to modulated triangular incommensurate lattices. The extent to which the effective interaction models treat the UIC solid should encourage the application of such models to other monolayer phases of Xe/Pt(111). An important extension of the calculations would be to identify what features of the interactions make the UIC phase of Xe/Pt(111) stable over such a large range of misfit.

A multiparameter interaction model for Xe/Pt(111) analogous to that used for Xe/Ag(111) appears to be lacking an important component of short-range repulsion and leads to distinctly smaller length scales than the effective interactions. The effects of adatom hybridization with the substrate²⁰ have not yet been incorporated in the model.

The general level of agreement of the modeling and the experimental data is an example of the ability to model physisorption phenomena using the methods of statistical mechanics.

ACKNOWLEDGMENTS

This work was supported in part by the National Science Foundation through Grant No. DMR-88-17761 and by the University of Wisconsin-Madison Graduate School with funds provided by the Wisconsin Alumni Research Foundation.

¹K. Kern, R. David, R. L. Palmer, and G. Comsa, *Phys. Rev. Lett.* **56**, 620 (1986).

²K. Kern, R. David, P. Zeppenfeld, and G. Comsa, *Surf. Sci.* **195**, 353 (1988).

³J. E. Black and P. Bopp, *Phys. Rev. B* **34**, 7410 (1986).

⁴J. E. Black and A. Janzen, *Langmuir* **5**, 558 (1989); *Surf. Sci.* **217**, 199 (1989); *Phys. Rev. B* **38**, 8494 (1988); **39**, 6238 (1989).

⁵J. M. Gottlieb, *Phys. Rev. B* **42**, 5377 (1990).

⁶J. M. Gottlieb and L. W. Bruch, preceding paper, *Phys. Rev. B* **44**, 5750 (1991) referred to as I.

⁷P. Bak, D. Mukamel, J. Villain, and K. Wentowska, *Phys. Rev. B* **19**, 1610 (1979).

⁸J. Villain and M. B. Gordon, *Surf. Sci.* **125**, 1 (1983).

⁹J. Cui and S. C. Fain, Jr., *Phys. Rev. B* **39**, 8628 (1989); H. Freimuth, H. Wiechert, H. P. Schildberg, and H. J. Lauter, *ibid.* **42**, 587 (1990).

- ¹⁰K. Kern, R. David, P. Zeppenfeld, R. Palmer, and G. Comsa, *Solid State Commun.* **62**, 391 (1987).
- ¹¹K. Kern, *Phys. Rev. B* **35**, 8265 (1987).
- ¹²B. Poelsema, L. K. Verheij, and G. Comsa, *Phys. Rev. Lett.* **51**, 2410 (1983); *Surf. Sci.* **152-153**, 851 (1985).
- ¹³P. Zeppenfeld, K. Kern, R. David, and G. Comsa, *Phys. Rev. B* **38**, 3918 (1988).
- ¹⁴K. Kern, R. David, R. L. Palmer, and G. Comsa, *Surf. Sci.* **175**, L669 (1986).
- ¹⁵L. W. Bruch and J. M. Phillips, *Surf. Sci.* **91**, 1 (1980).
- ¹⁶D. S. Bethune, J. A. Barker, and C. T. Rettner, *J. Chem. Phys.* **92**, 6847 (1990).
- ¹⁷C. R. Arumainayagam, R. J. Madix, M. C. McMaster, V. M. Suzawa, and J. C. Tully, *Surf. Sci.* **226**, 180 (1990); J. C. Tully, *Faraday Disc. Chem. Soc. London* **80**, 291 (1985); *Surf. Sci.* **111**, 461 (1981); E. K. Grimmelmann, J. C. Tully, and E. Helfand, *J. Chem. Phys.* **74**, 5300 (1981).
- ¹⁸B. L. Hall, D. L. Mills, P. Zeppenfeld, K. Kern, U. Becher, and G. Comsa, *Phys. Rev. B* **40**, 6326 (1989).
- ¹⁹W. A. Steele, *Surf. Sci.* **36**, 317 (1973).
- ²⁰J. E. Müller, *Phys. Rev. Lett.* **65**, 3021 (1990).
- ²¹L. W. Bruch, P. I. Cohen, and M. B. Webb, *Surf. Sci.* **59**, 1 (1976).
- ²²Y. Larher, *J. Chim. Phys.* **65**, 974 (1968); *J. Colloid Interface Sci.* **37**, 836 (1971).
- ²³G. L. Price and J. A. Venables, *Surf. Sci.* **59**, 509 (1976).
- ²⁴W. A. Steele, *The Interaction of Gases with Solid Surfaces* (Pergamon, Oxford, 1974).
- ²⁵J. M. Phillips, L. W. Bruch, and R. D. Murphy, *J. Chem. Phys.* **75**, 5097 (1981).
- ²⁶L. W. Bruch, *Surf. Sci.* **125**, 194 (1983), and references cited therein.
- ²⁷G. Schönhense, *Appl. Phys. A* **41**, 39 (1986).
- ²⁸J. Unguris, L. W. Bruch, E. R. Moog, and M. B. Webb, *Surf. Sci.* **109**, 522 (1981).
- ²⁹A value -520 K obtained in an unpublished work, cited in Ref. 12, was based on the smaller dipole moment μ_0 known for Xe/Ag(111), Refs. 15 and 21.
- ³⁰J. M. Phillips and L. W. Bruch, *J. Chem. Phys.* **83**, 3660 (1985).
- ³¹K. Kern (private communication).
- ³²L. W. Bruch, J. M. Gay, and J. Krim, *J. Phys. (Paris)* **46**, 425 (1985), and references cited therein.
- ³³F. F. Abraham, *Adv. Phys.* **35**, 1 (1986); M. Schöbinger and F. F. Abraham, *Phys. Rev. B* **31**, 4590 (1985).